

# AN ANALYSIS OF CRACK PROPAGATION BEHAVIOR IN STRESS CORROSION CRACKING UNDER REPEATING LOAD BY USING AN ASYMMETRICAL INTERNAL FRICTION MODEL

K. Nakasa\*, H. Itoh\*\* and H. Takei\*

\*Faculty of Engineering, Hiroshima University, Higashi-hiroshima, Japan  
\*\*Hiroshima Institute of Technology, Hiroshima, Japan

## ABSTRACT

The superposition of repeating load on the static load resulted in the decrease of crack propagation velocity in stress corrosion induced hydrogen cracking, and two peaks appeared on the relation between decreasing rate of crack propagation velocity and frequency. An asymmetrical internal friction model, which was proposed by assuming the asymmetrical interaction between hydrogen atoms and the cyclic moving of triaxial stress position near crack tip, well explained the existence of two peaks.

## KEYWORDS

Stress corrosion cracking; superposition of repeating load; decreasing crack propagation velocity; internal friction model; hydrogen atoms; cyclic moving of triaxial stress position.

## INTRODUCTION

Stress corrosion cracking of high strength steels in aqueous environment is divided mainly into two processes: (1) hydrogen adsorption and invasion into metal, and (2) hydrogen diffusion and concentration to the position with triaxial tensile stress ahead of crack tip. Although these processes are not changed substantially by the superposition of repeating load, both the crack growth initiation and crack propagation lives are greatly influenced. According to previous results (Nakasa and co-workers, 1977), the crack growth initiation time and the threshold stress intensity factor  $K_{Isc}$  are largely decreased by the superposition of repeating load, probably because the corrosion reaction is activated by the destruction of protective film on crack surface.

The crack propagation velocity is, on the other hand, decreased by the superposition of repeating load (Nakasa and co-workers,

1977, 1978, 1979, 1981), and the relation between decreasing rate of crack propagation velocity,  $1-\beta$ , and frequency,  $f$ , is expressed by a curve with two peaks. As the same behavior is also observed on the specimens hydrogen precharged (Nakasa and co-workers, 1984a), where only the hydrogen diffusion and concentration process controls crack propagation, it is concluded that the decrease of crack propagation velocity by the superposition of repeating load and the existence of two peaks on  $1-\beta$  vs.  $f$  curve are connected with the diffusion and concentration process of hydrogen atoms.

In the present paper, an quantitative analysis is attempted by using an asymmetrical internal friction model to explain the stress wave shape dependency of  $1-\beta$  vs.  $f$  curve observed in the previous study (Nakasa and co-workers, 1981).

### EXPERIMENTAL RESULTS

The decreasing rate of crack propagation velocity in stress corrosion cracking by the superposition of repeating load,  $1-\beta$ , is expressed as:

$$1-\beta = \frac{(da/dt)_s - (da/dt)_R}{(da/dt)_s}, \quad (da/dt)_s = f \cdot \int_N da/dt[K(t)]dt \quad (1)$$

where  $(da/dt)_R$  is the crack propagation velocity in stress corrosion cracking under repeating load and  $(da/dt)_s$  is that under static load, which can be calculated by graphical method (Wei and Landes, 1969) by assuming that the crack propagation under repeating load occurs in quite the same manner as under static load. When the range of stress intensity factor  $\Delta K$  is small compared with the mean value of repeating  $K$ ,  $K_m$ , or stress ratio  $R=K_{min}/K_{max}$  is large,  $(da/dt)_s$  is nearly equal to the crack propagation velocity at static  $K_m$ .

The example of  $1-\beta$  vs.  $f$  curve obtained on the low alloy Ni-Cr-Mo steel (JIS-SNCM439 steel; 0.40% C, 1.74% Ni, 0.76% Cr, 0.23% Mo) quenched and tempered at 473K is shown in Fig. 1. It is clear that two peaks appear in both sinusoidal and square load shapes, where  $\eta$  is the ratio of the time during

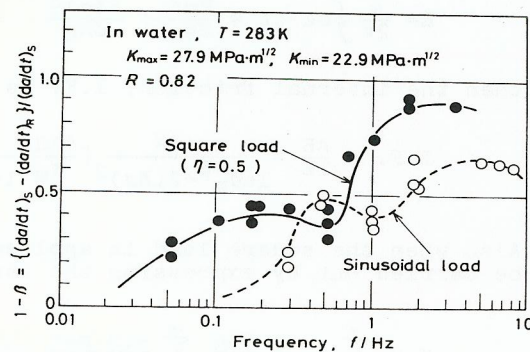


Fig. 1. Relation between decreasing rate of crack propagation velocity  $1-\beta$  and frequency (Nakasa and co-workers, 1981).

which  $K$  is held at maximum value,  $T_{max}$ , to one period,  $T_0$ , in square load shape. The reason why two peaks appear on  $1-\beta$  vs.  $f$  curve is closely connected with the facts that an incubation time appear after the quick load change and the incubation time after  $K$  is increased,  $t_u$ , is much shorter than that after  $K$  is decreased,  $t_d$  (Nakasa and co-workers, 1976, 1981, 1984b). This suggests not only that the position with triaxial tensile stress (triaxial position, for short) at crack tip moves with the change of  $K$  and the delay of diffusion and concentration of hydrogen atoms occurs, but also that the triaxiality or the stress gradient as a driving force for hydrogen diffusion is much smaller when  $K$  is decreased than when  $K$  is increased, because the plastic region formed when  $K$  is increasing is compressed by the elastic region around when  $K$  is decreasing.

Figure 2 schematically shows the interaction between hydrogen atoms (many points) and the cyclic moving of triaxial position (solid lines), where a microcrack is assumed to nucleate when a certain value of hydrogen concentration is achieved at the triaxial position: When frequency  $f$  is very low (at  $f_a$ ) or very high (at  $f_e$ ), hydrogen atoms can almost perfectly follow the moving of triaxial position or can not follow at all, respectively, so that the dispersion and the delay of concentration of hydrogen atoms do not occur at both frequencies, i.e.

$1-\beta \approx 0$ . When  $f=f_b$ , hydrogen atoms can easily follow the moving of triaxial position when  $K$  is increasing (from left to right), but not perfectly when  $K$  is decreasing (from right to left). In the latter period, the dispersion of hydrogen atoms occurs because dislocations and microvoids in grain or grain boundary trap the hydrogen atoms and prevent hydrogen atoms from diffusing with the same velocity, i.e. the concentration of hydrogen atoms is delayed and  $1-\beta > 0$ . When  $f=f_d$ , on the other hand, the perfect delay of hydrogen atoms when  $K$  is decreasing results in rather sufficient concentration of hydrogen atoms as at  $f=f_e$ , but the imperfect follow of hydrogen atoms when  $K$  is increasing causes the dispersion and delay of concentration of hydrogen atoms, i.e.  $1-\beta > 0$ . Thus, the first peak at  $f=f_b$  and the second peak at  $f=f_d$  correspond to the dispersion of hydrogen atoms during the processes when  $K$  is decreasing and  $K$  is increasing, respectively.

The existence of above asymmetrical interaction can be

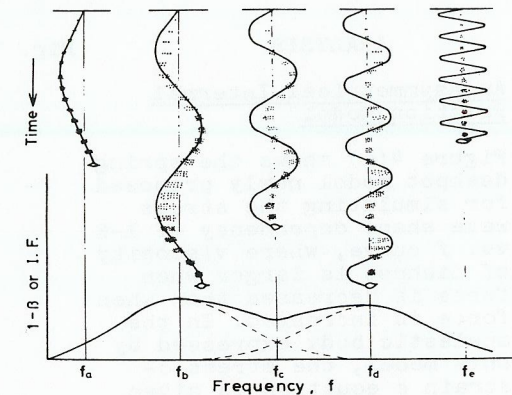


Fig. 2. Schematic interaction between hydrogen atoms and cyclic moving of triaxial position (Nakasa and co-workers, 1981).

ascertained by the experiment where the asymmetrical stress wave shape is used. Fig. 3 indicates the relations between  $1-\beta$  and  $f$  under square load with various values of  $\eta (=T_{max}/T_0)$ . As  $\eta$  decreases, two peaks approach and combine to one, i.e. the asymmetry of  $1-\beta$  can be canceled by the superposition of the asymmetrical stress wave.

ANALYSIS

An Asymmetrical Internal Friction Model

Figure 4(a) shows the spring-dashpot model newly proposed for simulating the stress wave shape dependency of  $1-\beta$  vs.  $f$  curve, where viscosity of dashpot is larger when force is decreased than when force is increased. In the anelastic body expressed by this model, the stress  $\sigma$ -strain  $\epsilon$  equation is given as:

$$\sigma + \tau_\epsilon \cdot \frac{d\sigma}{dt} = M_R (\epsilon + \tau_\sigma \cdot \frac{d\epsilon}{dt}) \quad (2)$$

where,  $\tau_\epsilon$  or  $\tau_\sigma$  is the relaxation time, which means the response speed of stress or strain when a constant strain or stress is applied quickly, and those after the force is decreased or increased are denoted as  $\tau_{\epsilon d}$ ,  $\tau_{\epsilon u}$  or  $\tau_{\sigma d}$ ,  $\tau_{\sigma u}$ , respectively.  $M_R$  is the elastic modulus after the relaxation is finished.

Next, when the external cyclic stress:

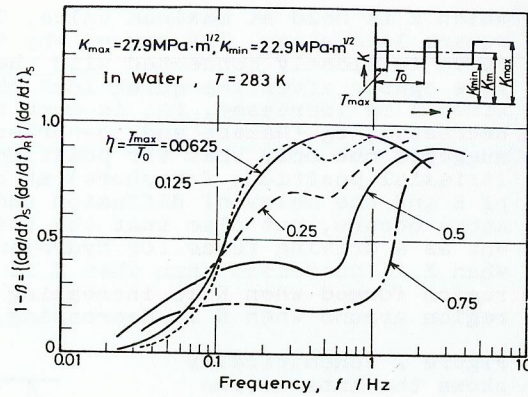


Fig. 3. Relations between decreasing rate of crack propagation velocity  $1-\beta$  and frequency under square load (Nakasa and co-workers, 1981).

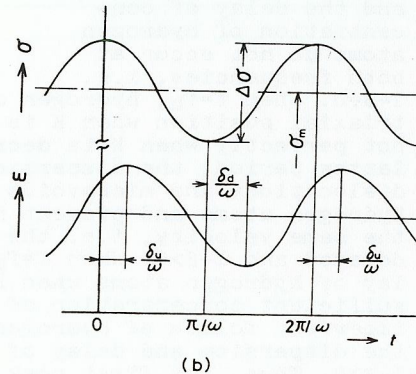
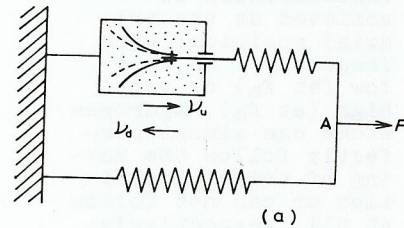


Fig. 4. (a): Spring-dashpot model, (b): deviation of phase in strain.

$$\sigma = \frac{\Delta\sigma}{2} \cos \omega t + \sigma_m \quad (3)$$

is applied to the anelastic body, where  $\Delta\sigma$  is range of stress,  $\sigma_m$  is mean stress,  $\omega$  is angular velocity, the strain is given by:

$$\frac{\delta_u}{\omega} \leq t \leq \frac{\pi}{\omega} + \frac{\delta_d}{\omega};$$

$$\epsilon = \epsilon_0 \cos(\omega t - \delta_d) + \epsilon_{md}, \quad \tan \delta_d = \frac{\omega \cdot \Delta\tau_d}{1 + (\omega \cdot \tau_d)^2},$$

$$\frac{\pi}{\omega} + \frac{\delta_d}{\omega} \leq t \leq \frac{2\pi}{\omega} + \frac{\delta_u}{\omega};$$

$$\epsilon = \epsilon_0 \cos(\omega t - \delta_u) + \epsilon_{mu}, \quad \tan \delta_u = \frac{\omega \cdot \Delta\tau_u}{1 + (\omega \cdot \tau_u)^2} \quad (4)$$

where the replacement,  $\tau_d = \sqrt{\tau_{\sigma d} \cdot \tau_{\epsilon d}}$ ,  $\tau_u = \sqrt{\tau_{\sigma u} \cdot \tau_{\epsilon u}}$ ,  $\Delta\tau_d = \tau_{\sigma d} - \tau_{\epsilon d}$ ,  $\Delta\tau_u = \tau_{\sigma u} - \tau_{\epsilon u}$ , is carried out. Thus, the deviation of phase in strain occurs as shown in Fig. 4(b), and the energy loss per one cycle,  $\Delta E$ , is calculated as:

$$\Delta E = \oint \sigma \cdot d\epsilon = \frac{\pi \Delta\sigma^2}{8M_R} \left[ \frac{\Delta\tau_d}{\tau_d} \cdot \frac{\omega \cdot \tau_d}{1 + (\omega \cdot \tau_d)^2} + \frac{\Delta\tau_u}{\tau_u} \cdot \frac{\omega \cdot \tau_u}{1 + (\omega \cdot \tau_u)^2} \right] \quad (5)$$

On the other hand, as the total energy per one cycle or the mean value of vibration energy  $E$  is:

$$E = \frac{\omega}{2\pi} \oint \sigma \epsilon \cdot dt = \frac{\sigma_m^2}{M_R} + \frac{(\Delta\sigma)^2}{8M_R} \quad (6)$$

then the internal friction, I.F. is given as:

$$I.F. = \frac{\Delta E}{2E} = \frac{\pi \cdot \Delta\sigma^2}{16\sigma_m^2 + 2(\Delta\sigma)^2} \left[ \frac{\Delta\tau_d}{\tau_d} \cdot \frac{\omega \cdot \tau_d}{1 + (\omega \cdot \tau_d)^2} + \frac{\Delta\tau_u}{\tau_u} \cdot \frac{\omega \cdot \tau_u}{1 + (\omega \cdot \tau_u)^2} \right] \quad (7)$$

Also when the square load is applied, the similar treatment can be carried out by expressing the stress  $\sigma$  as Fourier series:

$$\sigma = \sum_{n=1}^{\infty} \sigma_n = \frac{2\Delta\sigma}{\pi} \sum_{n=1}^{\infty} \frac{\sin n\pi\eta}{n} \cos n\omega t + \sigma_m + \frac{2\eta-1}{2} \Delta\sigma \quad (8)$$

From the response of strain  $\epsilon_n$  to  $\sigma_n$ , the energy loss  $\Delta E_n$  and the total energy  $E_n$  per one cycle for  $n$ -wave can be calculated, and the internal friction for square load can be obtained:

$$I.F. = \sum_{n=1}^{\infty} \frac{\pi \left(\frac{\Delta\sigma}{\sigma_m}\right)^2 \cdot \frac{\sin^2 n\pi\eta}{n}}{\left[n\pi^2 \left(1 + \frac{2\eta-1}{2} \frac{\Delta\sigma}{\sigma_m}\right)^2 + \left(\frac{\Delta\sigma}{\sigma_m}\right)^2 \frac{2\sin^2 n\pi\eta}{n}\right]} \times \left[ \frac{\Delta\tau_{dn}}{\tau_{dn}} \frac{n\omega\tau_{dn}}{1+(n\omega\tau_{dn})^2} + \frac{\Delta\tau_{un}}{\tau_{un}} \frac{n\omega\tau_{un}}{1+(n\omega\tau_{un})^2} \right] \quad (9)$$

By considering the triaxial (hydrostatic) tensile stress  $\sigma_t$  and the volumetric strain  $\epsilon_v$  at crack tip instead of  $\sigma$  and  $\epsilon$  in the above anelastic body, the internal friction model can be physically connected with the interaction model. Namely,  $\sigma_t = 1/3 \cdot (\sigma_x + \sigma_y + \sigma_z)$  is proportional to the stress intensity factor  $K$ , so that  $\Delta\sigma$  and  $\sigma_m$  in eqs. (7) and (9) can be replaced by  $\Delta K$  and  $K_m$ . In addition, if the microscopic crack nucleates at the triaxial position when a certain amount of hydrogen atoms concentrate to achieve a certain value of volumetric strain, the delay of concentration of hydrogen atoms due to the interaction causes the delay of attainment to critical volumetric strain, which introduces the delay of crack propagation velocity. Thus, the internal friction, I.F. is related to the decreasing rate of crack propagation velocity  $1-\beta$  although the experimental  $1-\beta$  consists of two factors:

$$1-\beta = (1-\beta)_1 + (1-\beta)_2, \quad (1-\beta)_1 = c \times I.F. \quad (10)$$

where  $c$  is a constant.  $(1-\beta)_2$  is the contribution of fatigue accumulation which can not be neglected at high frequency range (Nakasa and co-workers, 1979), and the next expression is assumed here for trial:

$$(1-\beta)_2 = k(1-R)(\log f - \log f_0), \quad f \geq f_0 \quad (11)$$

where  $k$  is a constant,  $f_0$  is the frequency from which the fatigue accumulation effect appears. In the present paper,  $k=2.8$ ,  $f_0=1$  Hz are used for sinusoidal wave shape, and  $k=1.95$ ,  $f_0=0.5$  Hz are adopted independently of  $\eta$  in square load shape for simplicity.

#### Relaxation Time

When the symmetrical internal friction ( $\tau_d = \tau_u$ ) occurs, the relaxation time is given by next form (Nakasa and coworkers, 1979):

$$\tau = \frac{\tau_0}{a_0} \cdot \frac{\Delta K \cdot K_m}{\sigma_{ys}^2} \exp\left(\frac{Q}{R_0 T}\right) \quad (12)$$

where  $a_0$  is lattice constant,  $\tau_0$  is a constant,  $\sigma_{ys}$  is yield strength (1.58 GPa for the material used),  $R_0$  is gas constant, and  $Q$  is the activation energy for hydrogen diffusion, respectively. Moreover, the activation energy obtained from the incubation time  $t_u$  or  $t_d$ , which appears after the quick increase or decrease of  $K_{min}$  ( $=22\text{MPa}\sqrt{m}$ ) to  $K_{max}$  ( $=28\text{MPa}\sqrt{m}$ ) or  $K_{max}$  to  $K_{min}$ , was about 21kJ/mol or 42kJ/mol (Nakasa and co-workers, 1984b). For the sinusoidal load shape, therefore, the next equation is assumed in the present paper to express the relaxation time when  $K$  is decreased,  $\tau_d$ , and that when  $K$  is increased,  $\tau_u$ :

$$\begin{pmatrix} \tau_d \\ \tau_u \end{pmatrix} = \frac{\tau_0}{a_0} \cdot \frac{\Delta K \cdot K_m}{\sigma_{ys}^2} \exp\left[\frac{(Q_0 - \lambda_0 K_m \pm \mu_0 \cdot \frac{\Delta K}{K_m})}{R_0 T}\right] \quad (13)$$

where  $Q_0$  is the activation energy when  $K$  is zero,  $\lambda_0$  and  $\mu_0$  are constants.

Similarly for the square load, the relaxation time  $\tau_{dn}$  or  $\tau_{un}$  in eq. (9) can be obtained by replacing  $\Delta K$  or  $K_m$  in eq. (13) with the range of stress intensity factor of  $n$ -wave,  $4\Delta K/\pi \cdot |\sin n\pi\eta|/n$  or mean value of  $K$ ,  $K_m + (2\eta-1)/2 \cdot \Delta K$  in eq. (8), respectively, because the square load wave is expressed as the summation of  $n$  series of sinusoidal waves with different stress amplitude.

#### Comparison of Calculation with the Experimental Results

For the calculation of eqs. (7), (9) and (13), the effective value of  $K$ ,  $K_{eff}$ , must be substituted, because the plastic zone at crack tip developed at  $K_{max}$  is compressed by the elastic zone around when  $K$  is decreased to  $K_{min}$  by  $\Delta K$ , and the actual triaxiality is much smaller than those anticipated from the nominal value of  $K_{min}$ . Thus, the next equation is proposed:

$$(K_{max})_{eff} = f(R) \cdot K_{max}, \quad (K_{min})_{eff} = g(R) \cdot K_{min} \quad (14)$$

where  $f(R)$  or  $g(R)$  is a function of stress ratio  $R$ . In the present paper,  $f(R)=1$ ,  $g(R)=R^4$ , and thus,  $(\Delta K)_{eff} = (K_{max})_{eff} - (K_{min})_{eff} = 17.6\text{MPa}\sqrt{m}$ ,  $(K_m)_{eff} = [(K_{max})_{eff} + (K_{min})_{eff}]/2 = 19.2\text{MPa}\sqrt{m}$  are adopted. Moreover, the constants in eqs. (7), (9), (10) and (13) were decided by referring the experimental data:  $c \cdot \Delta\tau_u/\tau_u = c \cdot \Delta\tau_d/\tau_d = 2.5$ ,  $\tau_0/a_0 = 0.0015\text{s/m}$ ,  $Q_0 = 41.8\text{kJ/mol}$ ,  $\lambda_0 = 418\text{(J/mol)}/\text{MPa}\sqrt{m}$ ,  $\mu_0 = 2.97\text{kJ/mol}$ . In eq. (9), the calculation was cut off at  $n=100$  by considering that the moving range of triaxial position corresponding to such a smaller  $n$  than 100 is comparable with the range of stress field around microvoid and dislocation and then the interaction or the dispersion of hydrogen atoms is difficult to occur. An example of calculated curves is shown in Fig. 5, which reveals relatively good coincidence with the experimental data. Fig. 6 shows the calculated  $(1-\beta)_1$  in each wave shape. By comparing this figure with the experimental relations (Fig. 3), it is clear that the asymmetrical internal friction model can well express the experimental tendencies.

## CONCLUSIONS

An asymmetrical internal friction model was proposed by assuming the existence of the asymmetrical interaction between hydrogen atoms and the cyclic moving of triaxial position. This model could well explain the following experimental results: (1) The crack propagation velocity in stress corrosion cracking is decreased by the superposition of repeating load and two peaks appear on the relation between frequency and decreasing rate of crack propagation velocity, (2) when the wave shape of superposed repeating load is square, both peaks approach and combine to one with decrease of  $\eta = T_{\max}/T_0$ , the ratio of the time during which the stress intensity factor  $K$  is kept at maximum value,  $T_{\max}$ , to one period,  $T_0$ , (3) the frequency at which two peaks appear is larger in sinusoidal load shape than in square load shape.

## REFERENCES

- Nakasa, K., H. Takei and T. Asamoto (1976). Trans. JIM **17**, 726-732.  
 Nakasa, K., H. Takei and M. Kido (1977). Eng. Fract. Mech. **9**, 867-877.  
 Nakasa, K., H. Takei and H. Itoh (1978). Eng. Fract. Mech. **10**, 783-793.  
 Nakasa, K., H. Takei and H. Itoh (1979). Eng. Fract. Mech. **11**, 689-702.  
 Nakasa, K., H. Takei and K. Kajiwara (1981). Eng. Fract. Mech. **14**, 507-517.  
 Nakasa, K., H. Takei, H. Itoh and M. Kobayashi (1984a). Jr. Japan Inst. Metals **48**, 136-143.  
 Nakasa, K., H. Itoh and H. Takei (1984b). Jr. Japan Inst. Metals **48**, 129-135.  
 Wei, R. P. and J. D. Landes (1969). Mat. Res. Std. **9**, 25-46.

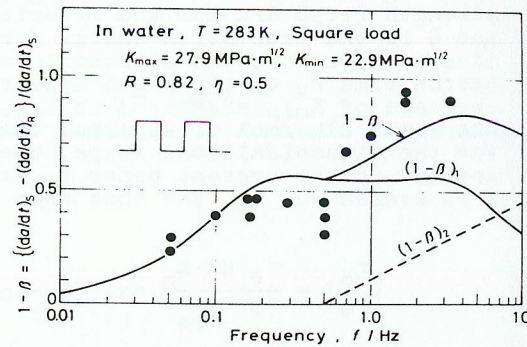


Fig. 5 Comparison between calculated and experimental relation between  $1-\beta$  and frequency.

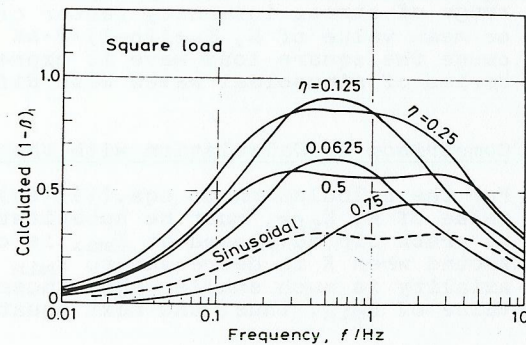


Fig. 6 Calculated relations between  $(1-\beta)_1$  and frequency.